Electronic Supplementary Material (ESI) for New Journal of Chemistry.

Supporting Information

Intramolecular Hydrogen Bond Directed Distribution of Conformational Populations in Derivatives of *N*'-benzylidenebenzohydrazide

Neeru Arya, Sandeep Kumar Mishra and N. Suryaprakash*

NMR Research Centre and Solid State and Structural Chemistry Unit, Indian Institute of Science, Bangalore 560012, India.

E-mail: nsp@iisc.ac.in; suryaprakash1703@gmail.com ; Fax: +91 8023601550; Tel: +91 8023607344; +91 80 22933300; +919845124802 (Cell)

Table of Contents

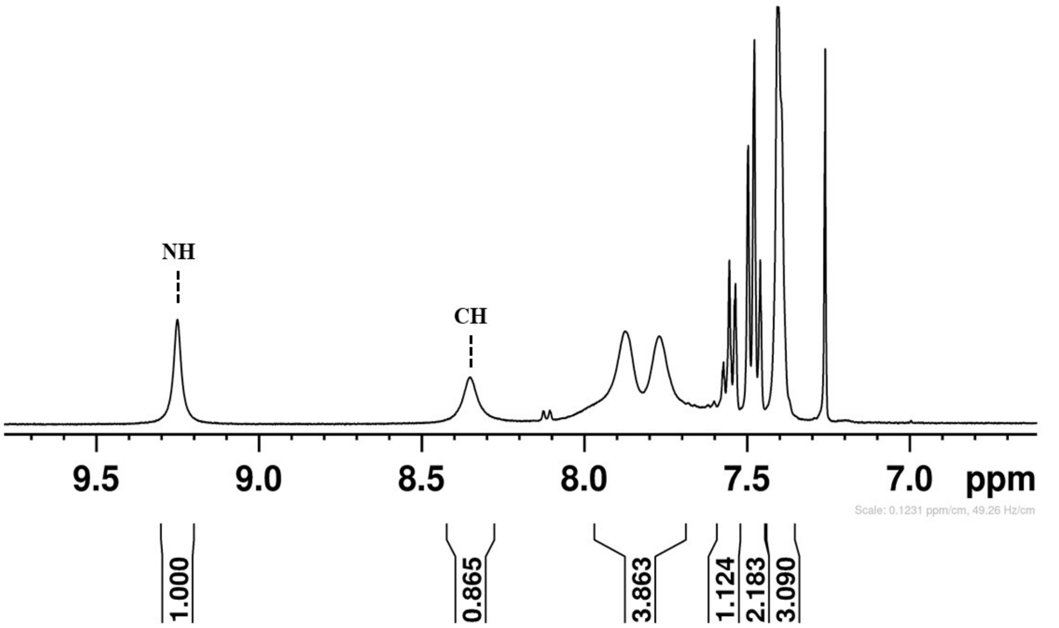

Figure S1. 400 MHz ^{1}H NMR spectrum of molecule **1** in the solvent $CDCl_3$ at 298K. NH imide and CH vinyl proton peaks are identified.

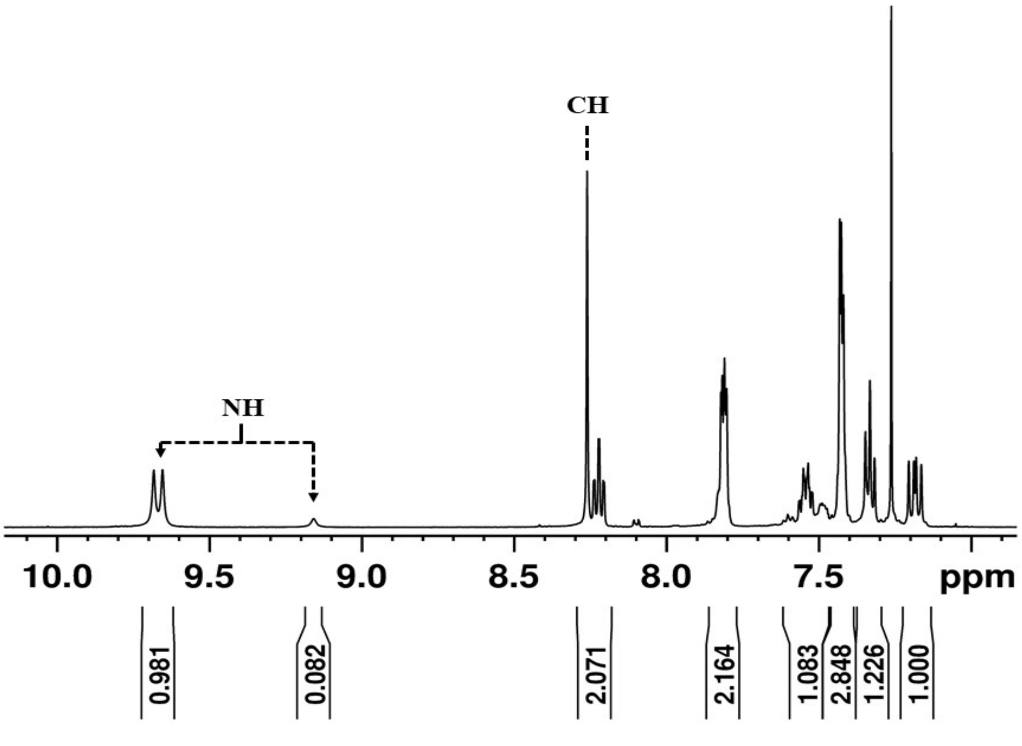

Figure S2. 400 MHz ^{1}H NMR spectrum of molecule **2** in the solvent $CDCl_3$ at 298K. NH imide and CH vinyl proton peaks are identified.

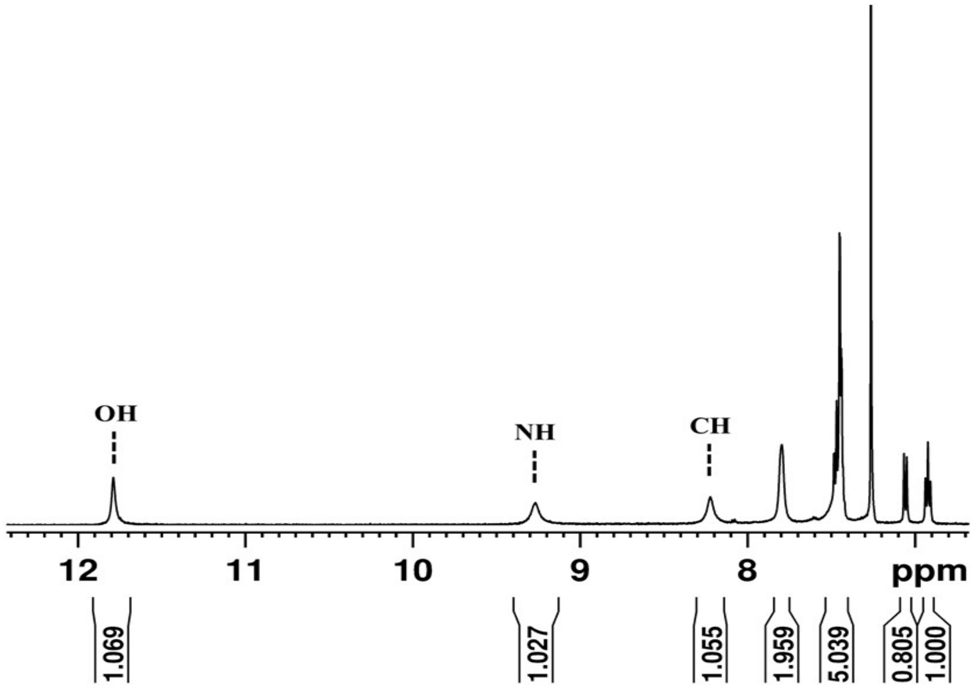

Figure S3. 400 MHz ^{1}H NMR spectrum of molecule **4** in the solvent $CDCl_3$ at 298K. NH imide and CH vinyl proton peaks are identified.

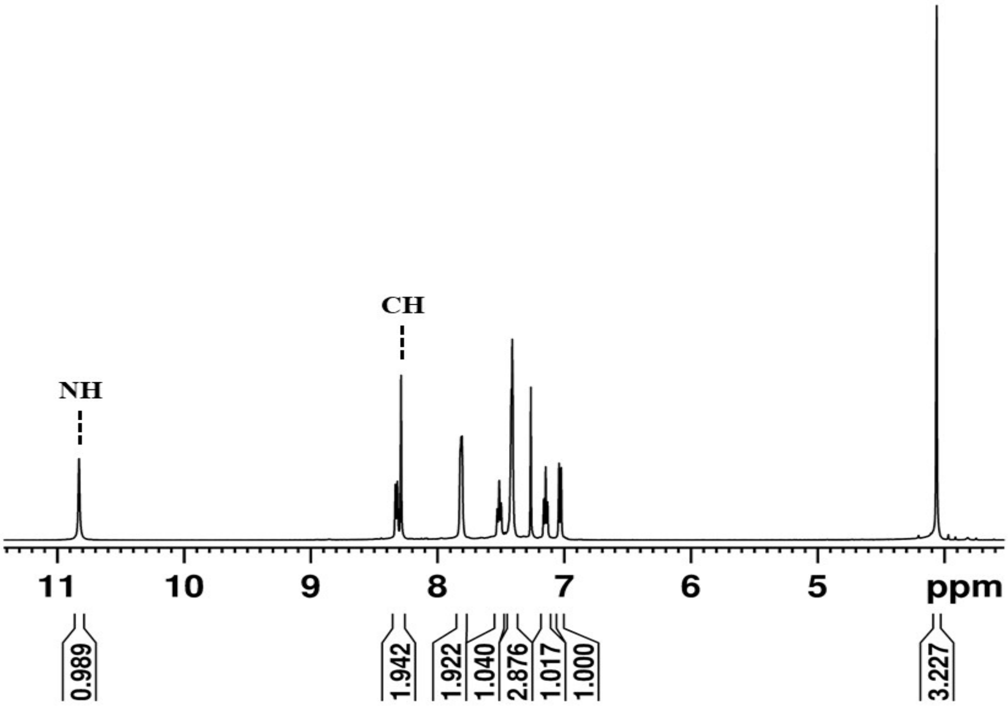

Figure S4. 400 MHz ^{1}H NMR spectrum of molecule **5** in the solvent $CDCl_3$ at 298K. NH imide and CH vinyl proton peaks are identified.

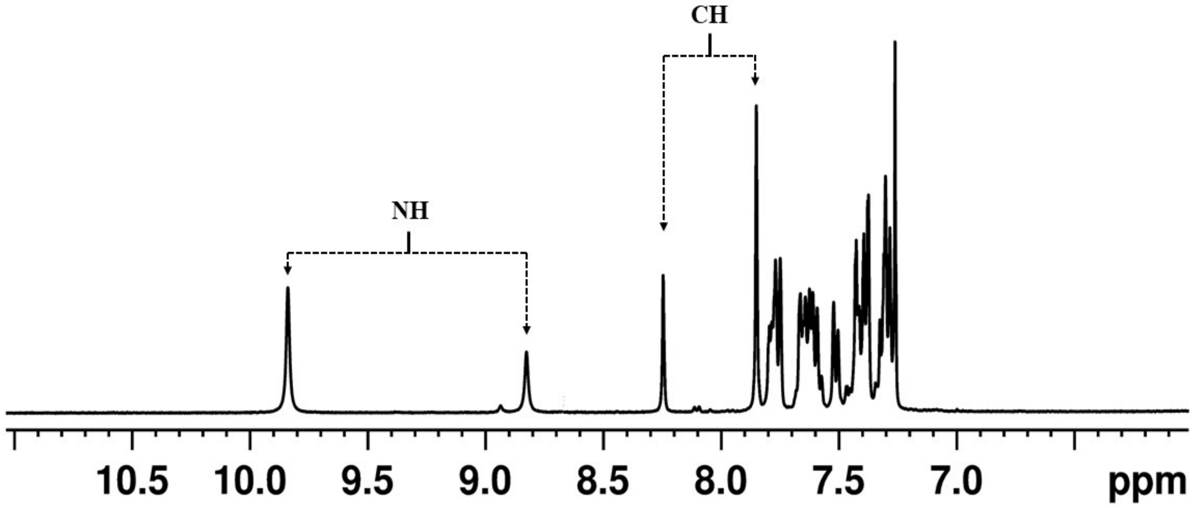

Figure S5. 400 MHz ^{1}H NMR spectrum of molecule **6** in the solvent $CDCl_3$ at 298K. NH imide and CH vinyl proton peaks are identified. Because of severe overlap of signals, the integral values are likely to be imprecise and hence not reported.

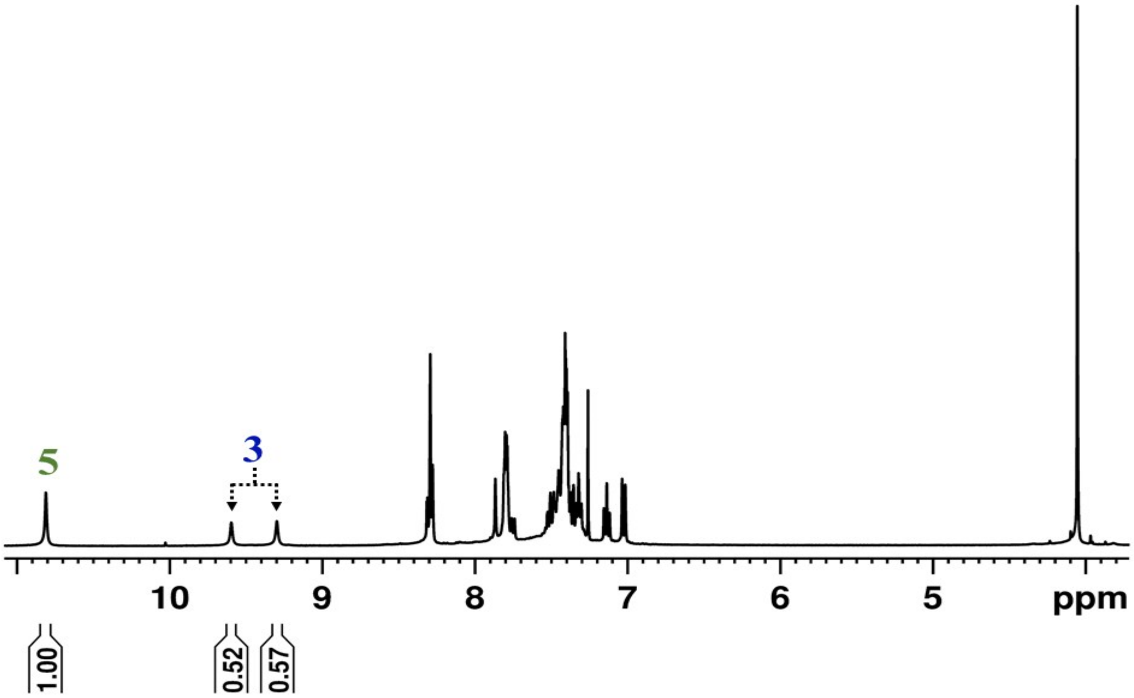

Figure S6. 400 MHz ^{1}H NMR spectrum for 1:1 ratio of molecules **3** and **5** in the solvent $CDCl_3$ at 298K. Peaks marked 3 and 5 are the NH proton peaks for molecules **3** and **5** respectively. From the visual inspection, it is evident that the NH peak of molecule **3** appears as two peaks with nearly half the intensities of NH peak of molecule **5**. However, the CH peaks cannot be identified due to severe signal overlap.

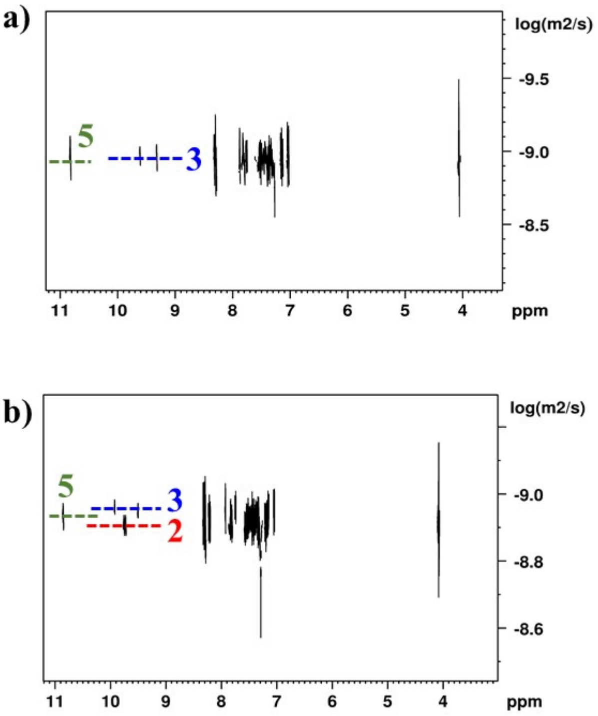

Figure S7. a) 400 MHz ^{1}H DOSY spectrum of 1:1 ratio of molecules **3** and **5**; b) 500 MHz DOSY spectrum of 1:1:1 ratio of molecules **2, 3** and **5** at 298 K in the solvent $CDCl_3$.

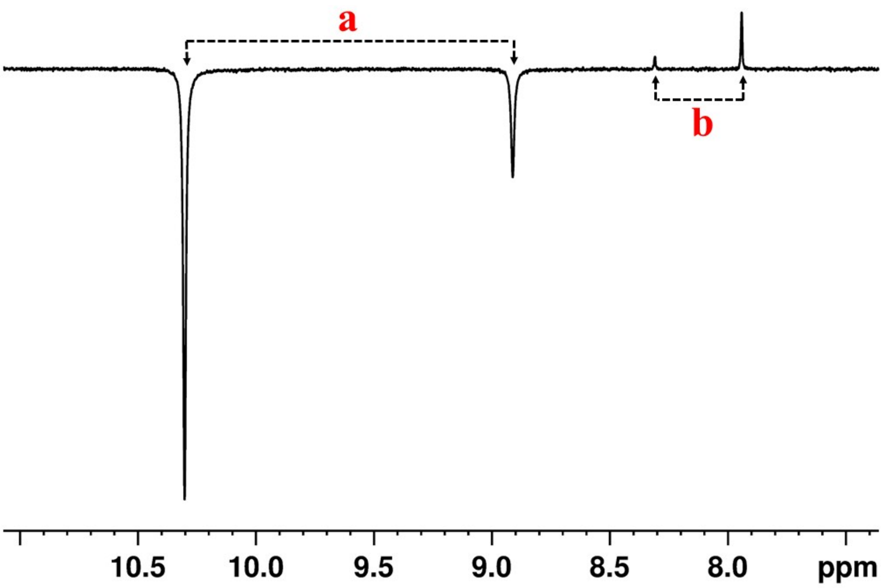

Figure S8. 400 MHz 1D difference NOE spectrum of molecule **6** in the solvent $CDCl_3$, at 298 K where the proton was selectively excited at 10.3 ppm. NH imide and CH vinyl proton peaks are identified by alphabets a and b respectively.

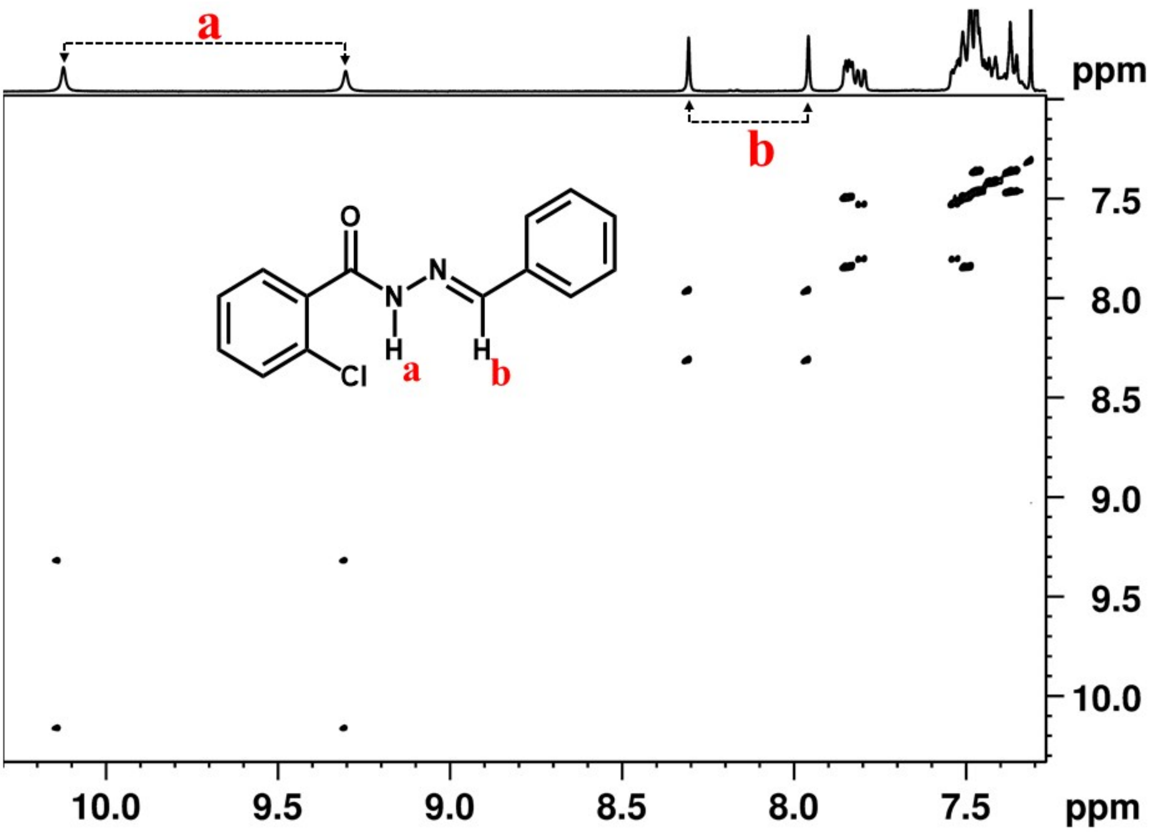

Figure S9. 400 MHz ^{1}H-^{1}H 2D-EXSY spectrum of molecule **3** in the solvent $CDCl_3$ at 298 K. NH imide and CH vinyl proton peaks are identified by alphabets a and b respectively.

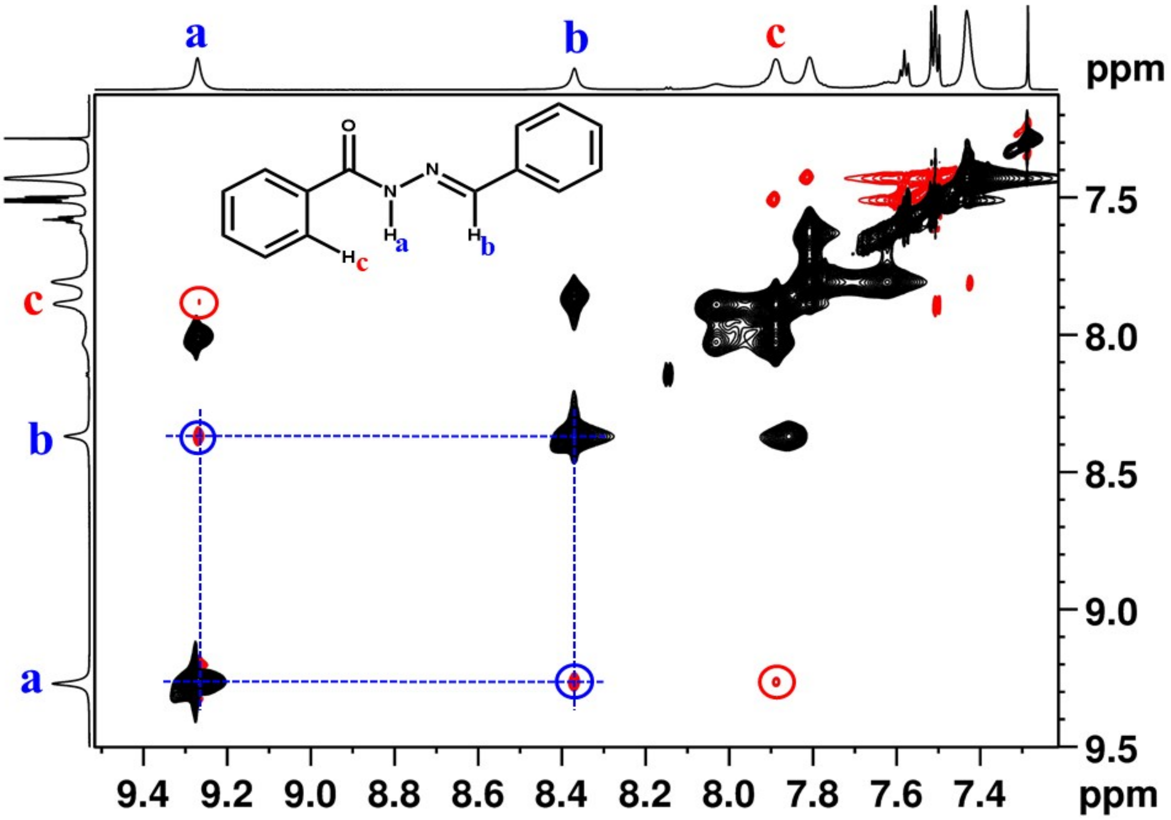

Figure S10: 800 MHz 2D ^{1}H-^{1}H NOESY spectrum of molecule **1** in the solvent $CDCl_3$ at 298 K. NH imide and CH vinyl proton peaks are identified by alphabets a and b respectively. The cross peaks between these protons (identified by blue circle) confirms that the molecules exist as *E* isomers with respect to C=N bond. And the cross peaks between aromatic proton H_c and imide NH proton H_a (identified by red circle) confirms that the molecules exist as *trans*, $E_{C\text{-}N}$ conformer

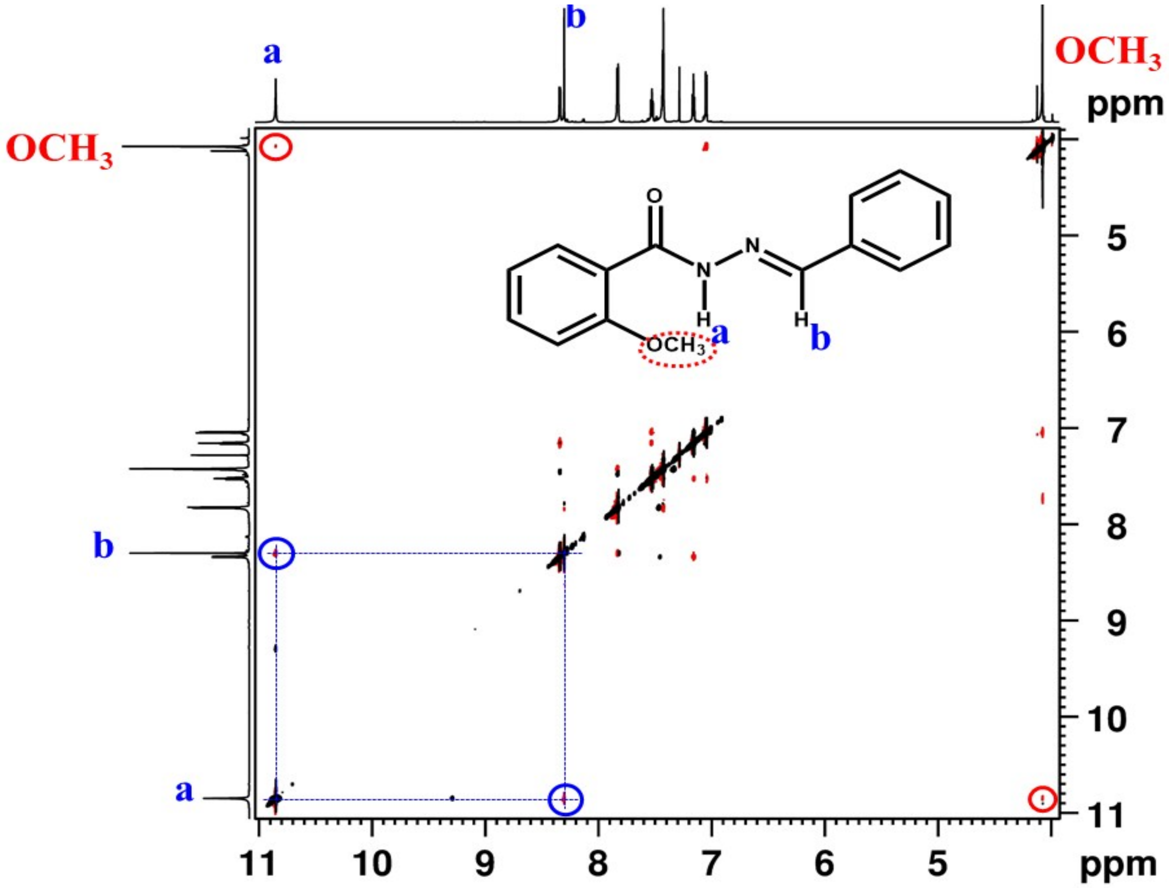

Figure S11: 800 MHz 2D ^{1}H-^{1}H NOESY spectrum of molecule **5** in the solvent $CDCl_3$ at 298 K. NH imide and CH vinyl proton peaks are identified by alphabets a and b respectively. The cross peaks between these protons (identified by blue circle) confirms that the molecules exist as *E* isomers with respect to C=N bond. And the cross peaks between methoxy substituent and imide NH proton (identified by red circle) confirms that the molecules exist as *trans*, $E_{C\text{-}N}$ conformer.

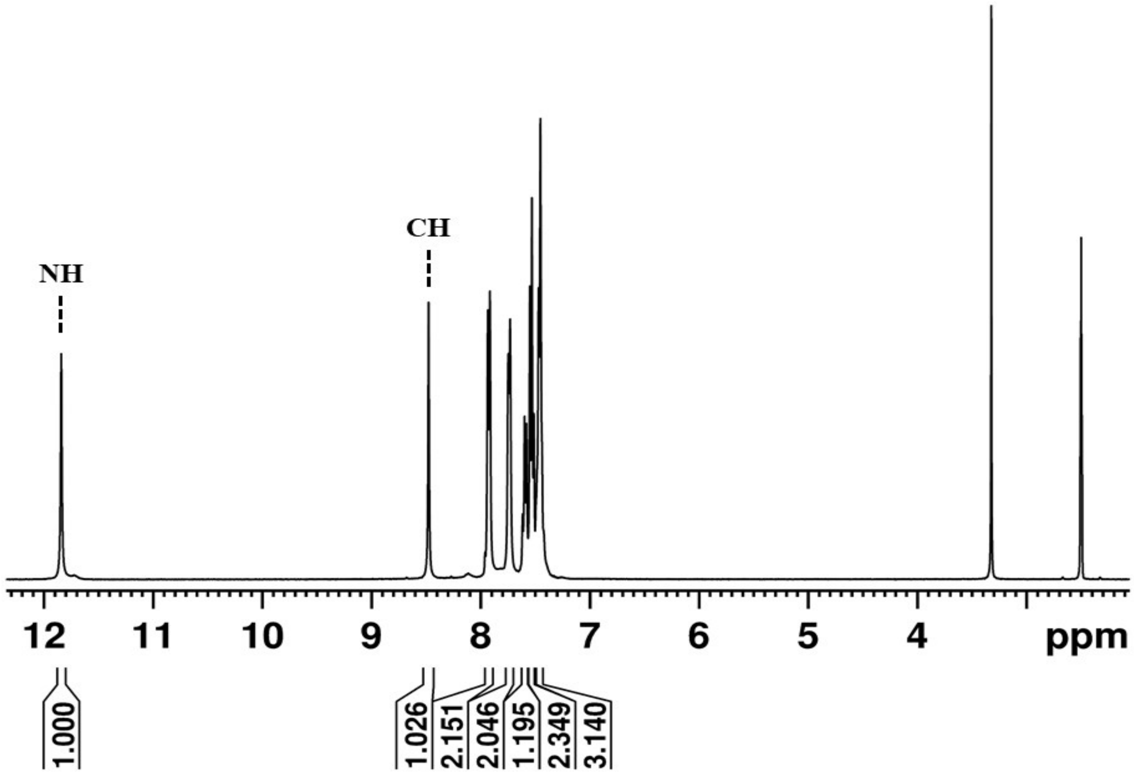

Figure S12. 400 MHz ^{1}H NMR spectrum of molecule **1** in the solvent DMSO at 298K. NH imide and CH vinyl proton peaks are identified.

.

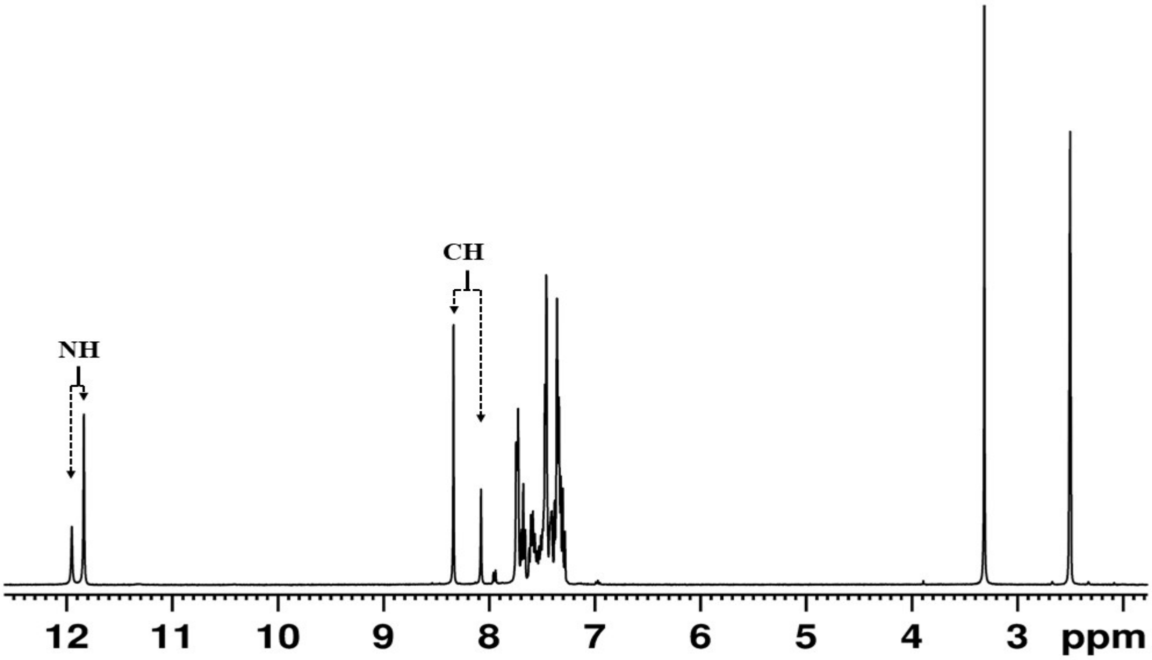

Figure S13. 400 MHz ^{1}H NMR spectrum of molecule **2** in the solvent DMSO at 298K. NH imide and CH vinyl proton peaks are identified. Because of severe overlap of signals, the integral values are likely to be imprecise and hence not reported.

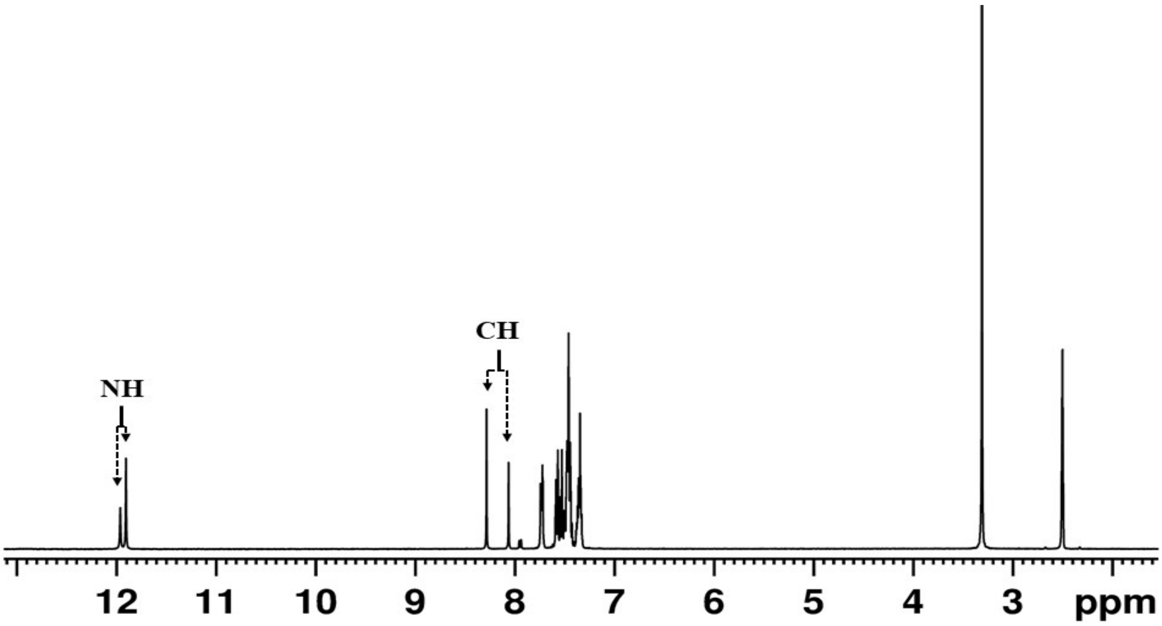

Figure S14. 400 MHz ^{1}H NMR spectrum of molecule **3** in the solvent DMSO at 298K. NH imide and CH vinyl proton peaks are identified. Because of severe overlap of signals, the integral values are likely to be imprecise and hence not reported.

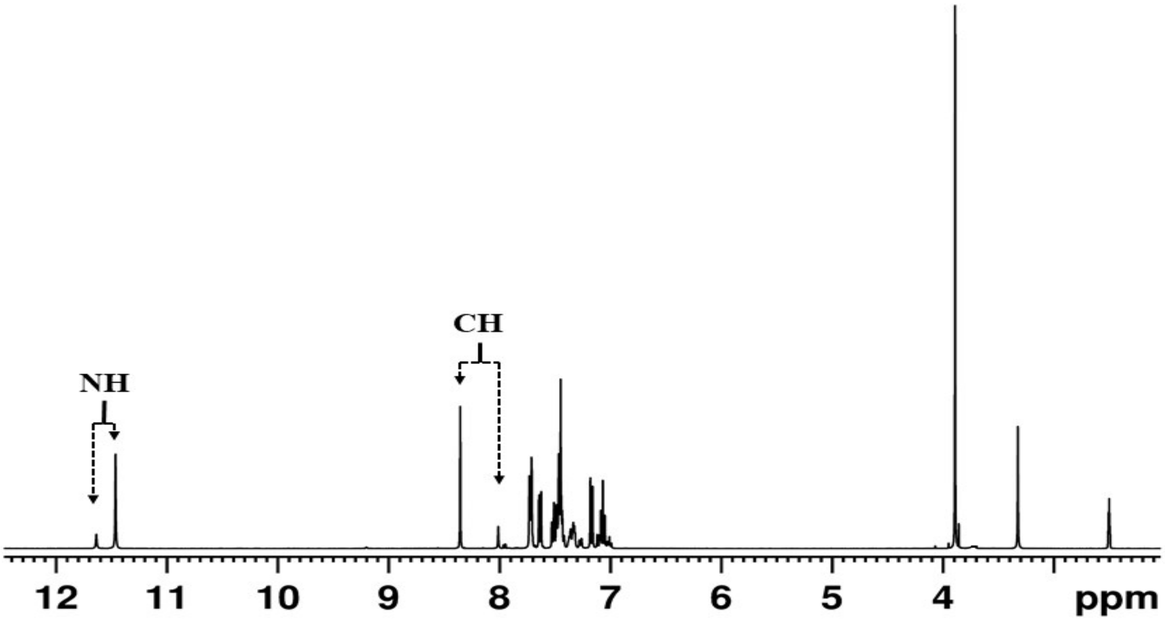

Figure S15. 400 MHz ^{1}H NMR spectrum of molecule **5** in the solvent DMSO at 298K. NH imide and CH vinyl proton peaks are identified. Because of severe overlap of signals, the integral values are likely to be imprecise and hence not reported.

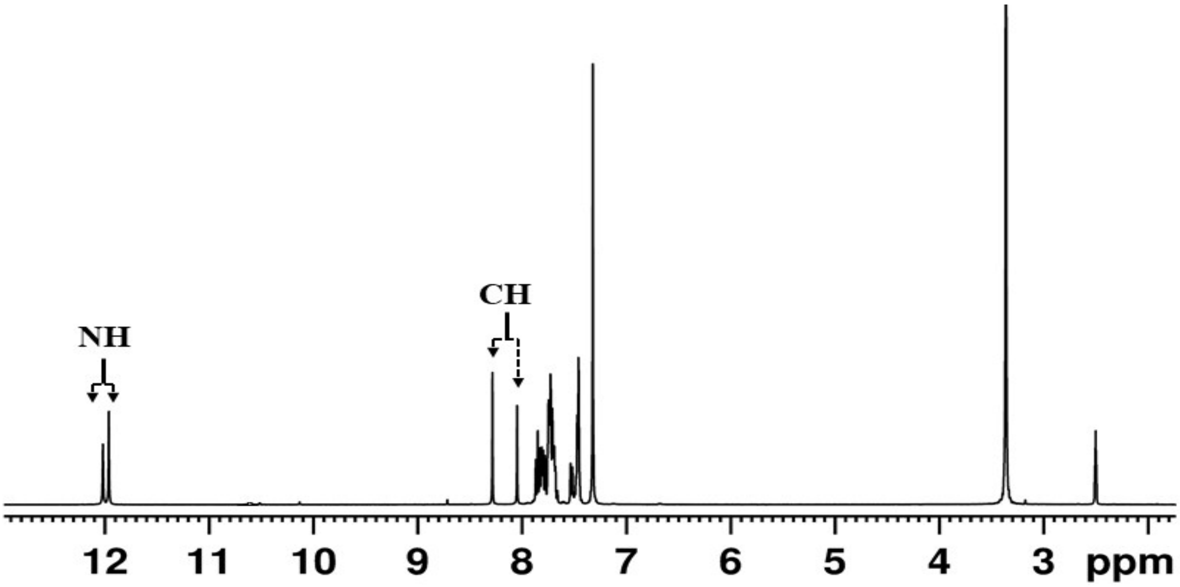

Figure S16. 400 MHz ^{1}H NMR spectrum of molecule **6** in the solvent DMSO at 298K. NH imide and CH vinyl proton peaks are identified. Because of severe overlap of signals, the integral values are likely to be imprecise and hence not reported.

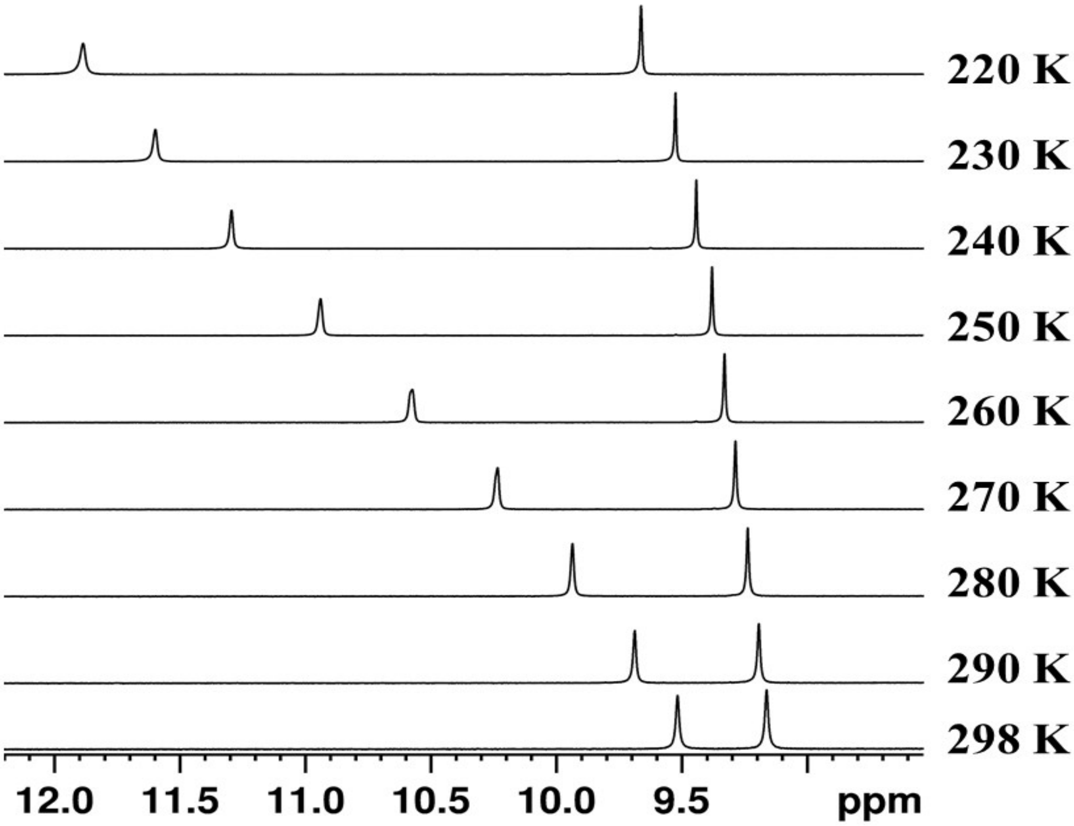

Figure S17. 400 MHz ^{1}H-NMR spectra of the selected NH regions of molecules **3** at different temperatures from 298 K to 220K (from bottom trace to top trace) in $CDCl_3$ solvent.

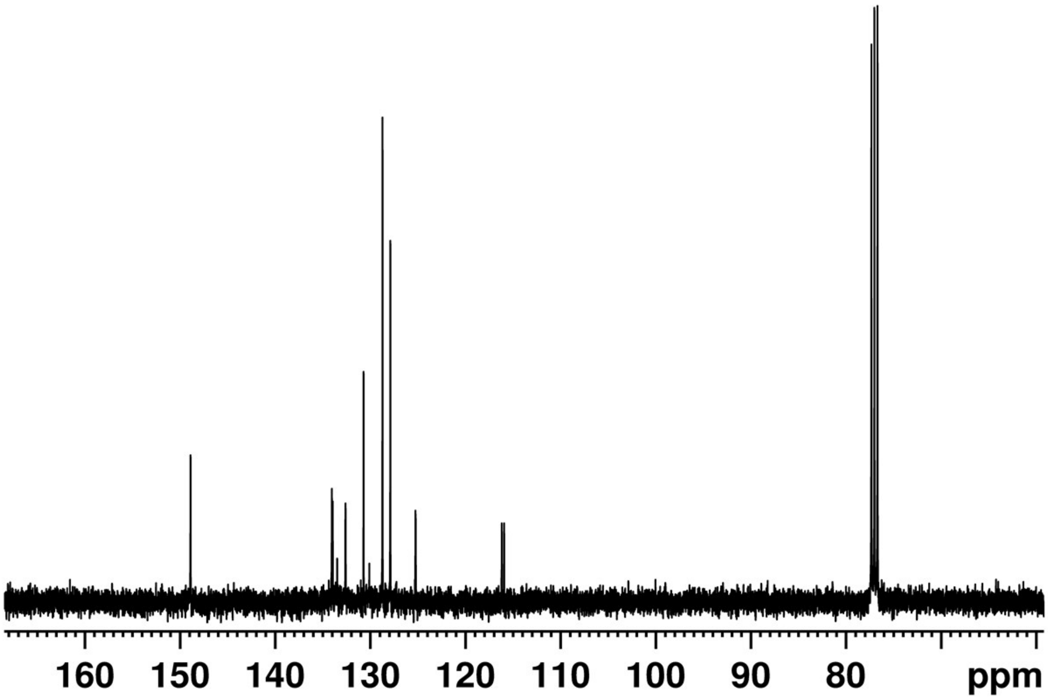

Figure S18. 400 MHz ^{13}C NMR spectrum of molecule **2** in the solvent $CDCl_3$ at 298K.

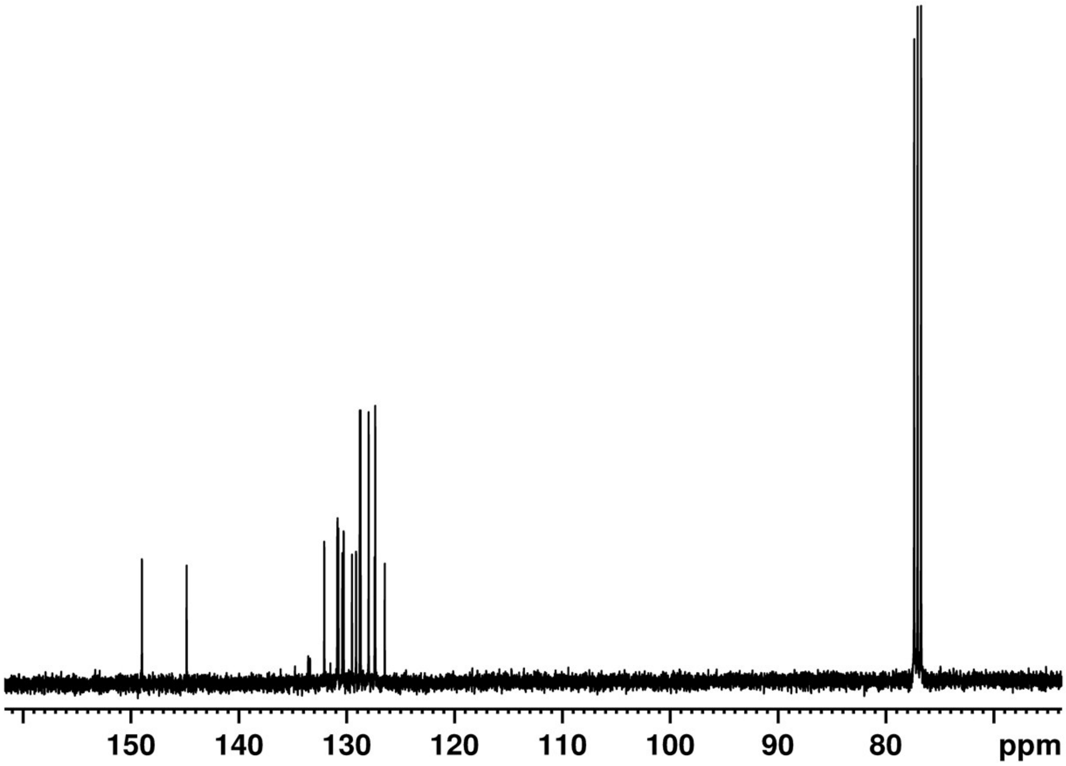

Figure S19. 400 MHz ^{13}C NMR spectrum of molecule **3** in the solvent $CDCl_3$ at 298K.

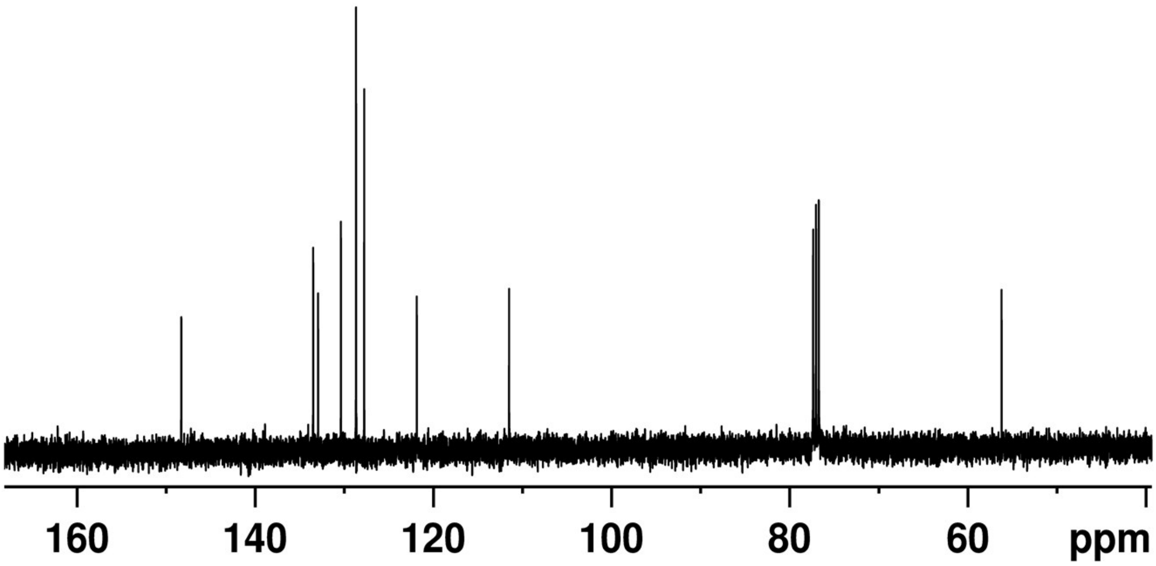

Figure S20. 400 MHz ^{13}C NMR spectrum of molecule **5** in the solvent $CDCl_3$ at 298K.

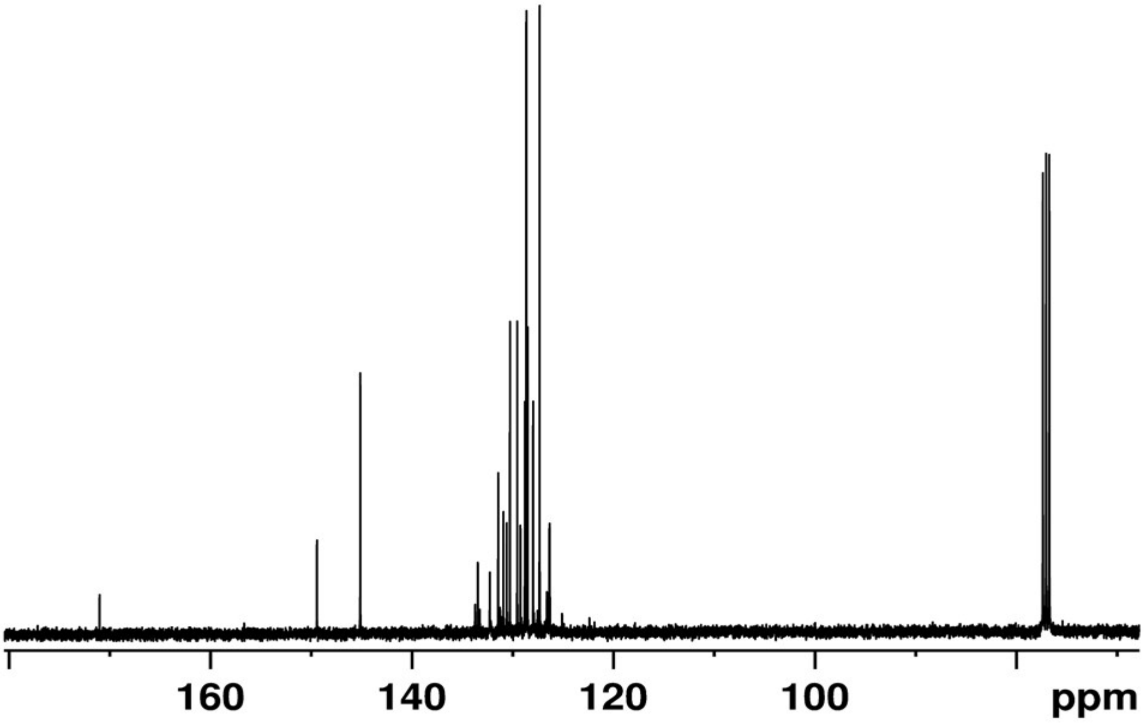

Figure S21. 400 MHz ^{13}C NMR spectrum of molecule **6** in the solvent $CDCl_3$ at 298K.

Theoretical computations

QTAIM Studies

Quantum theory of atoms in molecules (QTAIM)[1-4] makes use of quantum observables electron density $\rho_{(r)}$ and energy density for HB determination. The presence of (3, -1) critical point, commonly known as Bond Critical Point (BCP) in between the bond path joining two atoms indicates that the two atoms are hydrogen bonded. The BCPs and the bond paths of all the investigated molecules for both the conformers **I** and **II** are reported in Fig. S22. The sign of the Laplacian of electron density ($\Delta^2\rho_{(r)}$) and the value of electron density ($\rho_{(r)}$) at the BCPs are of great significance in determining the types and the strengths of HBs. Since there is no (X---N-H) intramolecular HB in conformer **II**, the magnitude of $\rho_{(r)}$ and the sign of $\Delta^2\rho_{(r)}$ for conformer **I** of molecules **2**, **3**, **5** and **6** are reported in Table S1.

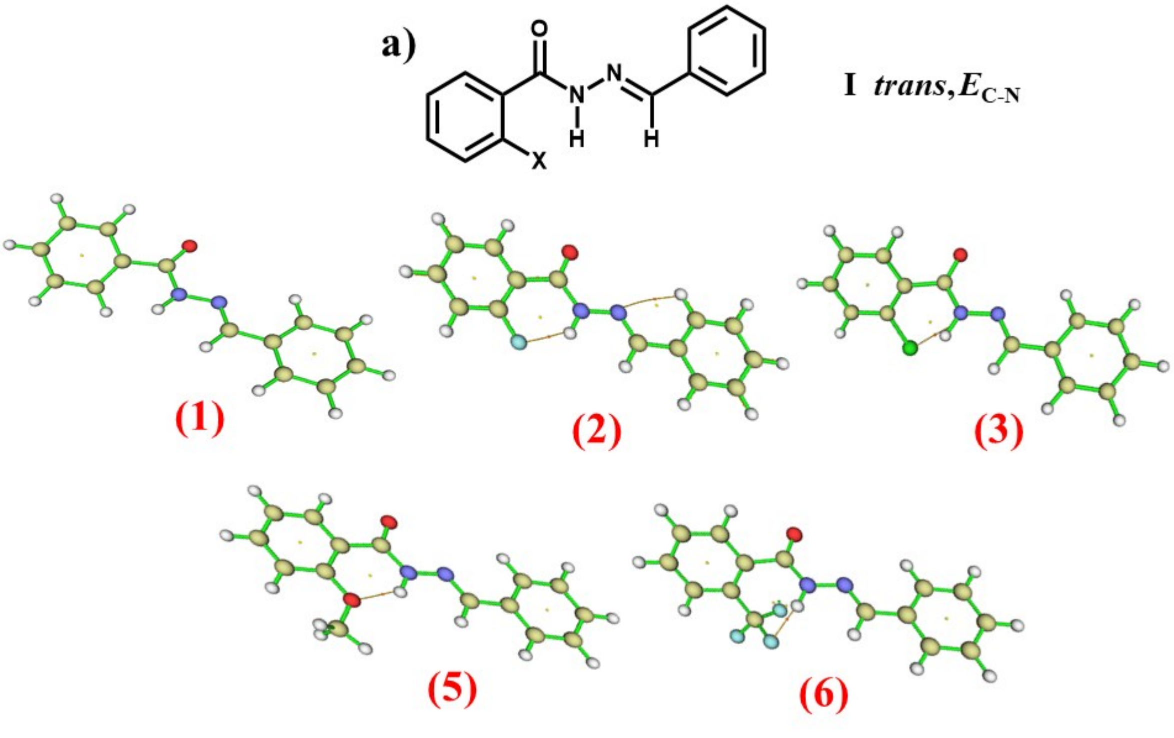

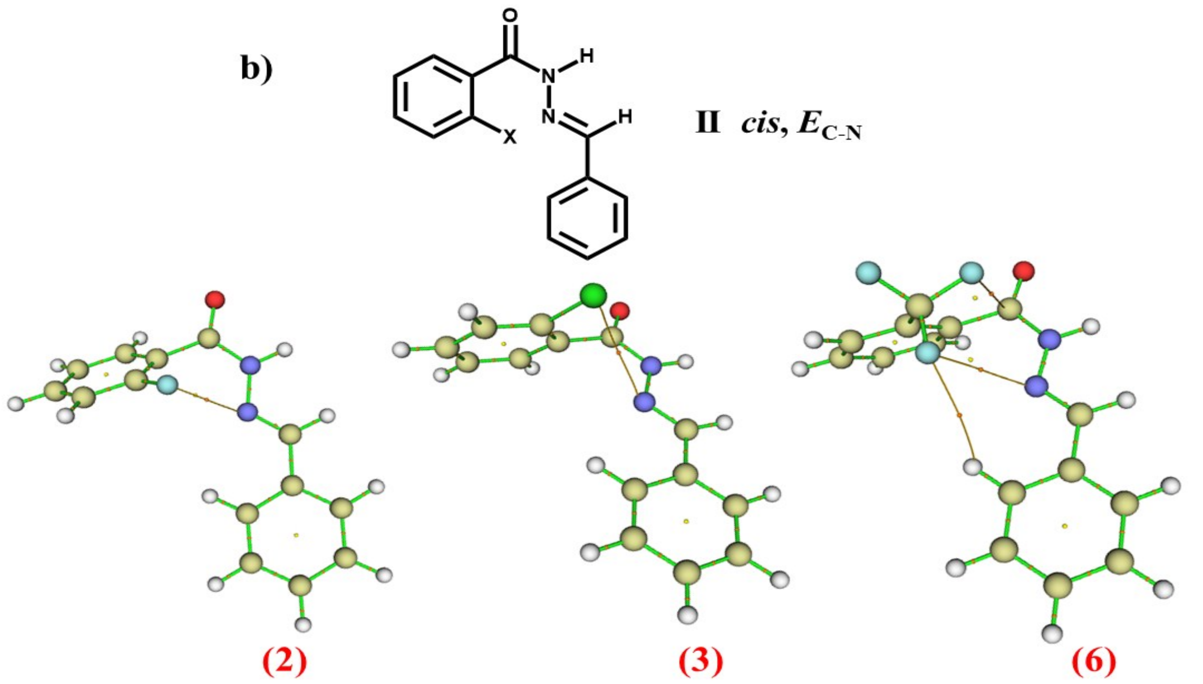

(2) (3) (6)

Figure S22. BCPs and bond paths a) for conformer **I** (*trans*, $E_{C\text{-}N}$) of molecules **1**, **2**, **3**, **5** and **6**; b) for conformer **II** (*cis*, $E_{C\text{-}N}$) of molecules **2**, **3** and **6**. Red dots indicate bond critical points and solid red line indicate the intramolecular HB.

Table S1. Values of Electron Density ($\rho_{(r)}$) and Laplacian of Electron Density ($\Delta^2\rho_{(r)}$) at (3, −1) BCPs of (X···HN) HBs for conformer **I** of molecules **2**, **3**, **5** and **6**.

Compound	**HB type (X---HN)**	**Electron Density ($\rho_{(r)}$) (au)**	**Laplacian of electron density ($\Delta^2\rho_{(r)}$)**
		I	**I**
2	(F---HN)	0.0153	0.0966
3	(Cl---HN)	0.0113	0.0435
5	(MeO---HN)	0.0319	0.1268
6	(CF_3---HN)	0.0137	0.0522

NCI studies

Non-covalent interactions (NCI) studies[5] based on the electron density and its derivatives are used as a visualisation tool for the identification of non-covalent interactions. The identification is done on the basis of the peaks that appear in the reduced density gradient (RDG) at low densities. The electron density ($\rho_{(r)}$) and the weak interaction forces show strong correlation giving negative and positive $\rho_{(r)}$ values for HBs and steric effects respectively. Whereas $\rho_{(r)}$ values for van der Waals interactions are very small (near to zero).[6] Grid points were calculated using the multiwfn program[7] and plotted for two functions, sign($\lambda_{(r)}$)$\rho_{(r)}$, as function 1 and reduced density gradient (RDG) as function 2 (Fig. S23).

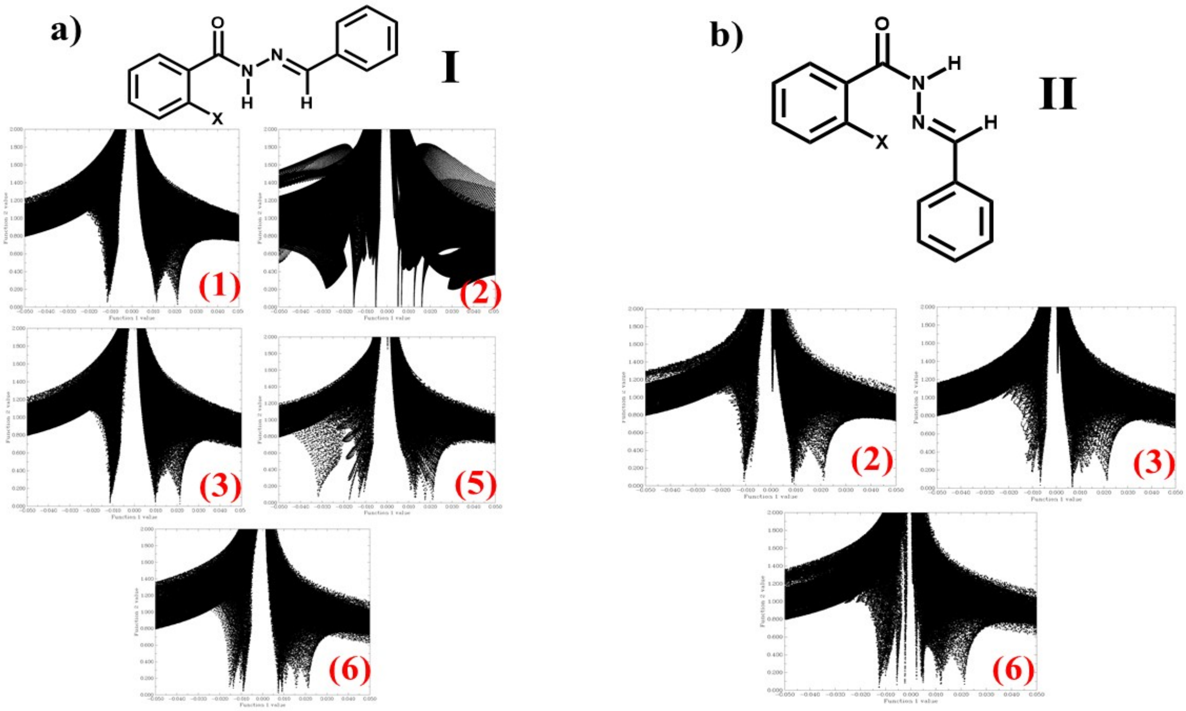

Figure S23. Plot of sign($\lambda_{(r)}$)$\rho_{(r)}$, as function 1 on X-axis and reduced density gradient (RDG) as function 2 on Y-axis a) for conformer **I** (*trans*, $E_{\text{C-N}}$) of molecules **1**, **2**, **3**, **5** and **6**; b) for conformer **II** (*cis*, $E_{\text{C-N}}$) of molecules **2**, **3** and **6**.

From the same grid points, colour-filled isosurfaces were also plotted for clear visualization of different type of interactions using VMD program[8] (Fig. S24). All the HBs are visualised as the green coloured isosurfaces whereas the red colour accounts for the steric hinderance due to phenyl rings and other HB mediated rings (Fig. S24).

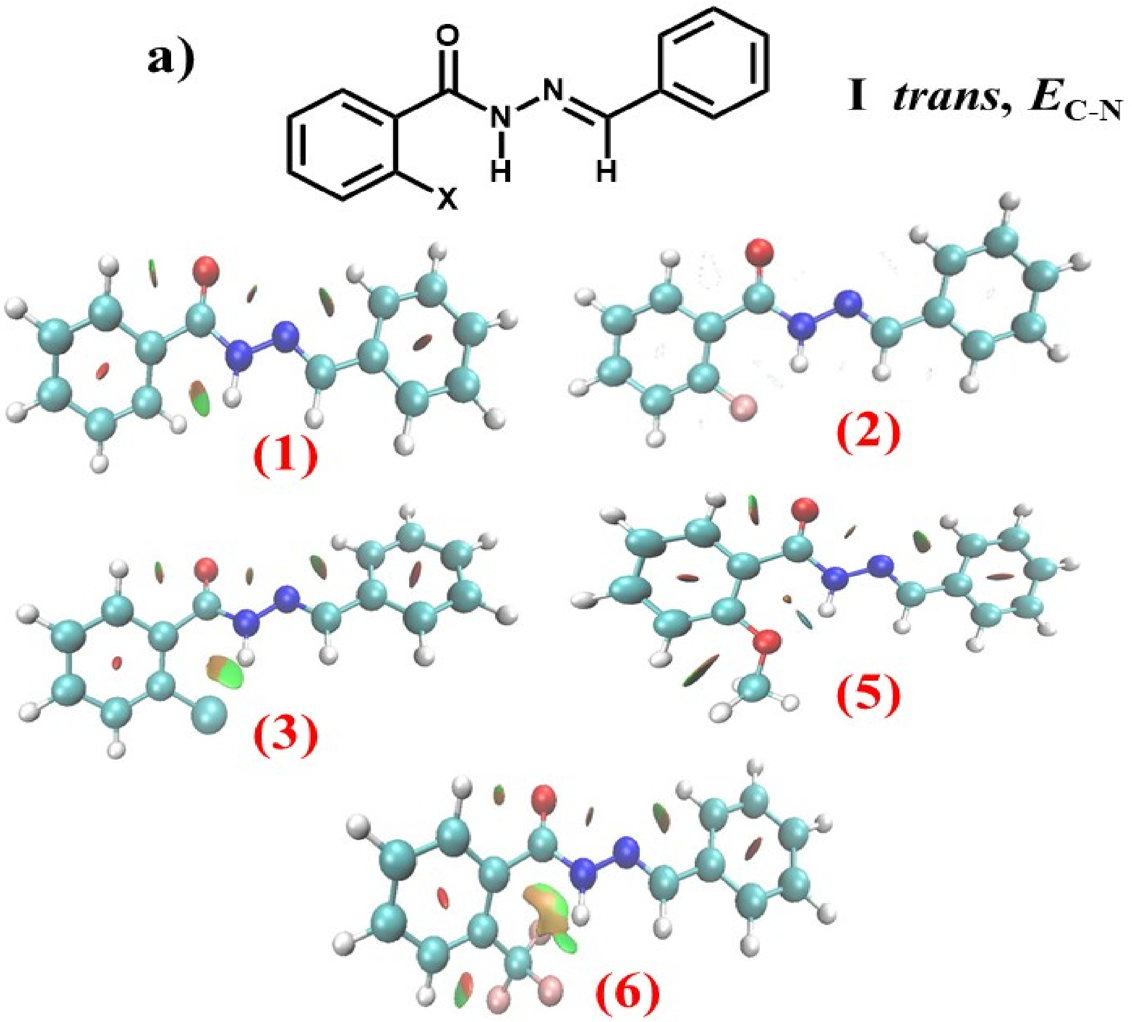

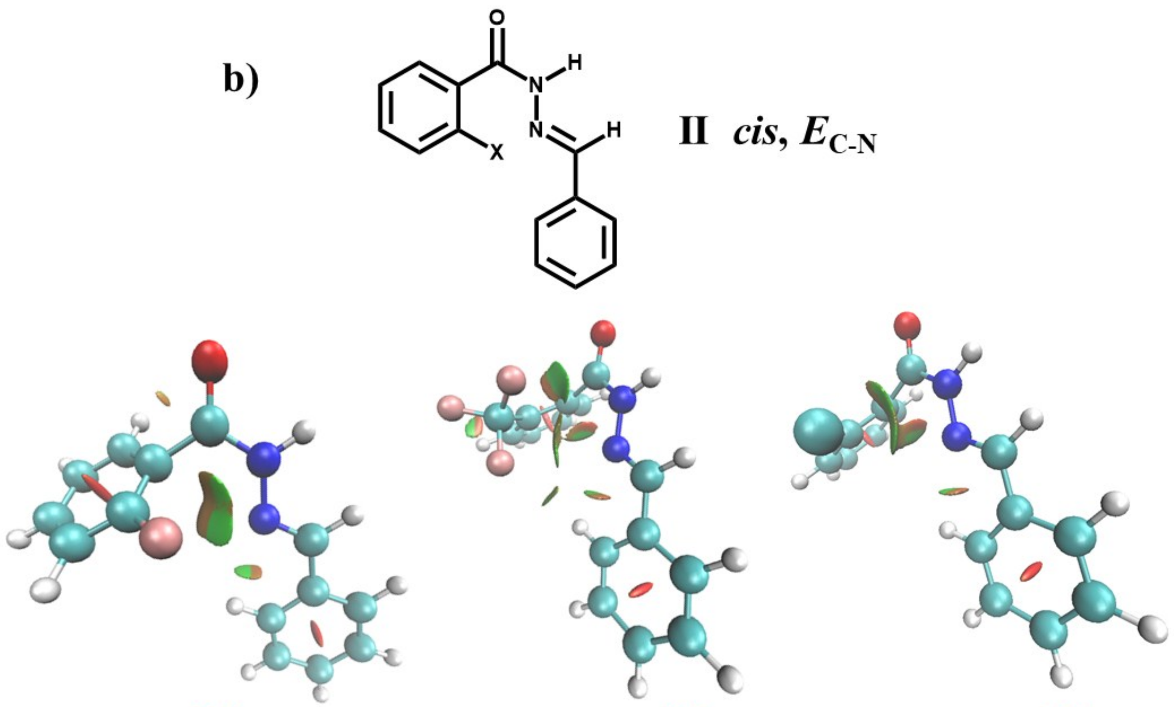

(2) (3) (6)

Figure S24. Coloured isosurface plots a) for conformer **I** (*trans*, $E_{C\text{-}N}$) of molecules **1**, **2**, **3**, **5** and **6**; b) for conformer **II** (*cis*, $E_{C\text{-}N}$) of molecules **2**, **3** and **6**. Green colour stands for HB and red colour denotes steric hindrance.

Experimental

All the NMR spectra were acquired on 400 and 800 MHz NMR spectrometers. TMS (tetramethylsilane) was used as the internal reference for both ^{1}H and ^{13}C NMR spectra. Deuterated $CDCl_3$ and DMSO-d_6 solvents were purchased and used as received. The characterization of all the synthesized molecules (**1-6**) was done by using various NMR experiments and ESI-MS technique. The available pulse programs in the library of NMR spectrometers were used for acquiring all the two-dimensional spectra, such as HSQC, NOSEY, COSY. Except for the temperature variation studies all other experiments were carried out at ambient temperature (298 K).

Synthesis procedure of N'-Benzylidenebenzohydrazide

Benzaldehyde and all the benzohydrazide derivatives were purchased and used as received. The X substituted benzohydrazide (1eq) was dissolved in chloroform and to it benzaldehyde (1 eq) was added drop by drop while stirring at $0^{0}C$. The mixture was kept on stirrer for 5-6 hours. The solvent $CHCl_3$ was evaporated using rotatory evaporator at a temperature and pressure of $50^{0}C$ and 500 mm Hg respectively. The white crude molecule left in RB was dissolved in 5 ml chloroform and was kept overnight for crystallization with addition of 0.1 ml of methanol.

ESI MS, Melting Point and Elemental Analysis

The melting point for all the studied molecules was measured for 3 different samples and the obtained range is reported.

Molecule 1:

ESI-MS $[M+H]^+$: Calculated for $C_{14}H_{12}N_2O$ 224.10 and found 224.10

Melting Point: 206-208°C.

Elemental Analysis: Calculated (%) for $C_{14}H_{12}N_2$: C 74.98, H 5.39, N 12.49; found C 74.99, H 5.16, N 12.20

Molecule 2:

ESI-MS $[M+H]^+$: Calculated for $C_{14}H_{11}FN_2O$ 243.09 and found 243.09

Melting Point: 125-126ºC.

Elemental Analysis: Calculated (%) for $C_{14}H_{11}N_2$: C 69.41, H 4.58, N 11.56; found C 69.28, H 4.36, N 11.51

Molecule 3:

ESI-MS $[M+H]^+$: Calculated for $C_{14}H_{11}ClN_2O$ [M+H]+ 259.06 and found 259.06

Melting Point: 165-167ºC.

Elemental Analysis: Calculated (%) for $C_{14}H_{11}N_2$: C 65.00, H 4.29, N 10.83; found C 65.19, H 4.08, N 10.99

Molecule 4:

ESI-MS $[M+H]^+$: Calculated for $C_{14}H_{12}N_2O_2$ 241.09 and found 241.09

Melting Point: 232-235ºC.

Elemental Analysis: Calculated (%) for $C_{14}H_{12}N_2$: C 69.99, H 5.03, N 11.66; found C 69.78, H 5.08, N 11.41

Molecule 5:

ESI-MS $[M+H]^+$: Calculated for $C_{15}H_{14}N_2O_2$ 255.11 and found 255.11

Melting Point: 180-182ºC.

Elemental Analysis: Calculated (%) for $C_{15}H_{14}N_2$: C 70.85, H 5.55, N 11.02; found C 70.37, H 5.38, N 10.94

Molecule 6:

ESI-MS $[M+H]^+$: Calculated for $C_{15}H_{11}F_3N_2O$ 293.09 and found 293.09

Melting Point: 158-159ºC.

Elemental Analysis: Calculated (%) for $C_{15}H_{11}N_2$: C 61.65, H 3.79, N 9.59; found C 61.28, H 3.57, N 9.35

References

1. W. Kohn and L. J. Sham, *Phys. Rev.*, 1965, **140**, A1133.
2. R. G. Parr and W. Yang, *Density-Functional Theory of Atoms and Molecules,* Oxford University Press, New York, 1989.
3. R. F. W. Bader, *Atoms in Molecules: A Quantum Theory*, Oxford University Press, Oxford, 1990.
4. N. S. Golubev, I. G. Shenderovich, S. N. Smirnov, G. S. Denisov and H.-H. Limbach, *Chem. Eur. J.*, 1999, **5**, 492.
5. R. F. W. Bader, S. G. Anderson and A. J. Duke, *J. Am. Chem. Soc.*, 1979, **101**, 1389−1395.
6. E. R. Johnson, S. Keinan, P. Mori-Sánchez, J. Contreras-García, A. J. Cohen and W. Yang, *J. Am. Chem. Soc.*, 2010, **132**, 6498–6506.
7. T. Lu and F. Chen, *J. Comput. Chem.,* 2012, **33**, 580–592.
8. W. Humphrey, A. Dalke and K. Schulten, *J. Mol. Graphics*, 1996, **14**, 33–38.